COATING IMBIBITION RATE STUDIES OF OFFSET INKS: a novel determination of ink-on-paper viscosity and solids concentration using the ink tack force-time integral.

P. A. C. Gane
Vice President Research & Development
Paper & Pigment Systems

J. Schoelkopf[1]
Senior Scientist

OMYA AG
CH-4665 Oftringen
Switzerland

G. P. Matthews
Reader in Applied Physical Chemistry

Environmental and Fluids Modelling Group
Department of Environmental Sciences
University of Plymouth
PL4 8AA Devon, U.K.

ABSTRACT

Comparison of visco-elastic structure relaxation of a presheared offset ink with observed ink tack development on both non-absorbent substrates, of different smoothness and surface free energy, and on a representative absorbent multi-coated paper is made. The methods used include oscillatory and shear rheometry, and the SeGan Ink Surface Interaction Tester (ISIT), respectively. By diluting the ink with mineral oil, a plot of viscosity against solids content could be established. The viscosity of the progressively diluted ink was then extrapolated back toward increasing concentration. In this way a relation was developed between the viscous character of the ink at a given concentration on the substrate, i.e. effectively the ink-on-paper viscosity and solids content, and the tack force measurement. The individual force-time integrals of the ISIT under constant separation acceleration, known as the ink tack pull-off curves during tack rise, could then be used to obtain a predicted volume loss of fluid from the ink on a real coated paper sample. The role of intrinsic ink/rubber blanket adhesion is assumed inherently as a continuous boundary condition, but the "sealing" effect at the substrate surface, which is dependent on ink amount, roughness and ink mobility, strongly influences the likelihood of cavitation. Cavitation, if present, is shown to contribute to the observed tack force, and occurs especially on very smooth and non-absorbent substrates. A model, previously proposed by Xiang and Bousfield, 1998, adopting a geometry of parallel plate separation in a fluid medium, is compared with the tack results. A considerable mismatch is found between the earlier model and the results obtained from the methodology in this current study. Better agreement is found using an analysis of the tack force-time integrals, footprint area and an uniaxial extensional viscous term from which an improved model of the tack-force mechanism is presented. This novel approach allows the solids and viscous parameters of the ink to be analyzed as the initial ink setting actually occurs on real papers.

Keywords: Ink tack, viscosity, printability, cavitation, ink rheology, offset printing, substrate absorption.

[1] Author to whom correspondence should be addressed

INTRODUCTION

The physical phenomena occurring during and after the application of printing ink in an offset print process are considered to be important factors in achieving desired print properties. Ink vehicle, the continuous liquid phase, is removed from the setting film by absorption into the porous paper coating surface. The dynamics of this absorption are observed as a build-up of internal ink tack (cohesion) from the shortest timescale of fractions of a second up to half a minute or longer, followed by a subsequent decay of ink surface tack (ink-blanket adhesion), often lasting up to an hour or in some cases days. The tack cycle of rise and decay is linked to properties of the final cured ink film, such as print gloss, press runnability and rub-resistance. The control of tack is therefore crucial for the multicolor offset printing process.

It is also important to recognize, that on a running press which has reached equilibrium, the ink retained on subsequent color blankets is aged both over time and in respect to tack. The tack of this blanket-retained ink has been built-up during multiple contacts with progressively setting ink as the print form makes many contacts with the paper. This aged ink cannot be simulated by fresh ink used in rapid timescale test methods. Therefore, tack must be studied over realistically long timescales before the equilibrium press condition can be simulated correctly. This is especially important when considering the dynamic absorption by coatings coming into contact with such aged ink.

In previous studies we investigated the mechanism of liquid absorption into coating pigment structures (1). We identified the relevance of inertial flow as physically predicted by Bosanquet (2) who expanded the well known Lucas Washburn (3) equation to contain the inertial effect of the liquid mass which has to be accelerated by the wetting force. A 3D plot shows that there exists a time dependent optimum for flow as a function of capillary radius. The consequence is that pores up to a given diameter in a porous network, this diameter being in turn a function of time, fill very fast while bigger features remain by-passed and tend to remain unfilled under conditions of limited supply volumes of fluid found in the case of thin applied ink films. This promotes what we call a preferential pathway flow (4). The existence of unfilled or by-passed pores is also known from soil science and study with micro models (5). Inertial flow in a glass capillary was observed by Quéré using a high speed camera (6). With modifications, we applied the Bosanquet equation to a sequential wetting algorithm for Newtonian fluids in a pore space simulator, Pore-Cor[2], previously developed and described in the literature (7).

Offset inks contain Newtonian liquids as solvents and extenders, but the rheology of the ink itself, especially as it interacts with the paper and the printing press, shows a visco-elastic behavior. The absorption process is itself complex as the porous paper coating structure does not imbibe the ink itself. The liquid phase, the so-called vehicle, is absorbed into the porous structure while the binder/pigment particles, due to size exclusion, remain on the surface, and solvated resins become adsorbed (8). This leads to an effective rise in viscosity of the ink and to a fast formation of an immobilized "filtercake" layer of binder and pigment particles on the coating surface and therefore to a decrease of mobile ink layer thickness (9).

In this work we combine methods of rheology to study the relaxation of presheared ink. An extrapolation of viscosity toward higher solids content is derived initially from viscosity data obtained under progressive dilution of the ink with mineral oil. This extrapolated viscosity as a function of increasing solids content is then compared with the observed ink tack rise as a function of time as measured on the SeGan Ink Surface Interaction Tester[3] (ISIT) to obtain potentially a predicted volume loss of fluid from the ink. The findings are first linked to measurements of the printed ink tack force development on different non absorbent substrates. This permits the analysis of the contribution from mechanisms of ink split, structural rebuild and cavitation. We then go further to analyze the influence of the mobile ink layer thickness as a function of time between printing and subsequent backsplitting on a typical offset paper. A model is then developed to describe the solids and viscous behavior of the ink under the controlled extensional acceleration conditions of the static point ISIT test. Thereby we correlate the single integrated force-time curves, each at a given time after printing, with a process extensional viscosity and hence, via the Trouton ratio, to the observed relaxing shear viscosity of the ink. This novel analysis provides a means of defining the important rheological characteristics of the ink in situ on the paper surface.

[2] Pore-Cor is a software program of the Environmental and Fluids Modelling Group, University of Plymouth, PL4 8AA, U.K.
[3] ISIT is a product name of SeGan Ltd., Perrose, Lostwithiel, Cornwall PL22 0JJ, England

THREE BASIC POST-PRINT MECHANISMS

The general framework of mechanisms of a process like printing is the same as for many applications where a multiphase suspension or dispersion is applied onto a solid surface which may be permeable and porous. The framework after initial application consists mainly of evaporation, absorption and curing.

Evaporation, a diffusive process, is dependent on vapor pressure and therefore strongly linked to temperature. The "escape" of volatile fluid molecules results in an increasing solids concentration at the liquid/vapor boundary; a skin formation is often observed.

Absorption on a fine porous substrate happens due to capillary forces where the Laplace pressure of the curved liquid menisci forms the driving force. Also non-Laplacian driven wetting is possible under all kinds of film flow situations. Furthermore, diffusion and effusion also contribute to absorption; the former relates to molecular or particulate transport into a non porous medium, e.g. a cured latex film, the latter is molecular and applies mainly to molecular mixing or exclusion. The consequence is an upconcetration of solid particles at the solid-liquid boundary by size exclusion effects. Even if the size of potential ink particles is much smaller than the mean capillary diameter it is likely that the ink particles block pore throats and junctions immediately (10) This increase in solids concentration is actually the build-up of a secondary porous layer, often with progressively reduced permeability due to small void spaces. Only in a potential final stage when liquid menisci are formed at the upper boundary of this filtercake does it start to act as a structure competing for liquid with the primary porous substrate.

Curing is a chemical process influencing often the later stages of the first two processes discussed above where the type of curing mechanism furthermore complicates this issue. Oxidative and humidity curing start from the boundary contact layer and are usable only for thin layer applications as access to the inner bulk is dependent on the diffusive permeability of the curing material. Light, from infrared to ultraviolet, electron beam (EB) and heat-induced curing also start at the exposed surface and continue depending on the permittivity of the medium. Only chemical curing, due to any kind of crosslinking or chainlinking reactions, starts everywhere in a medium at a given concentration. The impact of curing is a steady further rise in viscosity and a potential change in temperature, as mentioned before, although it may be only at surfaces exposed to the curing "starter". If this starter is oxygen, it happens in every capillary the polymer fluid enters or remains during the entry of air. The final impact then is the ongoing formation of a network structure resulting in an immobilization and solidification of the former fluid thus reducing the stickiness or adhesional properties.

In this work we focus on the offset or lithographic print process where, after the initial pressure impulse applied to both sides of the paper from the printing nip, the above-mentioned three main mechanisms become active in the tackification and setting of an offset ink. Capillary forces and diffusion, plus limited evaporation later in the sequence of heatset web offset, remove the fluid phase from the applied ink layer causing a progressive concentration of solids towards the boundary between ink and the surface of the porous substrate. The curing, mainly oxidative, occurs ideally after the removal of the fluid components resulting in a solidification of the ink film involving polymerization and setting of resin binder components in the ink formulation. Previous work has shown that the bundle of capillary tubes model is insufficient to model the absorption process. Applying the Lucas-Washburn (LW) equation, assuming a simple bundle of capillaries, often leads to an unrealistic dimension of the effective pore radius and contradicts observation when comparing ink setting on fine gloss coating structures with those of coarser matte coatings. The classical equation of Bosanquet (2) which was virtually ignored for many years since its inception in 1923, includes the effect of inertial retardation of the liquid as it becomes accelerated into the larger pores. Inertia promotes a regime of flow that is linear with respect to time in comparison to the square root linearity of the LW equation. While this effect in straight capillaries is detectable using high speed cameras it was considered not to be relevant because of the short timescale of its influence, i.e. ~10 ns for water into a capillary of diameter > 0.1 µm. In contrast, the effect in a porous network is proposed to be additive. In each single feature of a porous network where the liquid is accelerated, inertia acts over a timescale similar to the pore filling time and leads to a differential in wetting front velocity and position during absorption between the finer and the larger pores. Interestingly, due to observed mass balance in experimental approaches on a macroscopic scale, a proportionality with respect to the square root of time is observed. This observation systematically led to the assumed verification of Poiseuille flow and hence Lucas-Washburn dynamics. However, this overlooked the remaining need for a defined effective capillary radius or surface energy relationship to describe the discrepancy regularly seen between absorption rates for fine and coarse structures, viz. fast ink

setting on fine pigmented glossy papers versus slow ink setting on matte papers made from coarse pigments. This issue is discussed further in some detail in recent publications (7), (4). High liquid viscosities shift the time of inertial flow into irrelevant short timescales and low densities decrease the effect of inertia. In the case of offset inks, where the fluid is formed from alkanes in a mineral oil fraction or vegetable oils, the viscosity is in the order of 0.5 - 40 mPas and the density in the order of 730 kgm^{-3}. These fluid properties maintain the relevance of the inertial timescale during the pore selection process within the porous network of a paper coating, i.e. the time taken to fill an isometric pore of, say, 0.1 µm or less, will be of the order of < 10 ns. During this time, larger pores fail to fill due to the inertial lag time of the fluid trying to enter them and so selection in favor of finer pores occurs within the constraints of the available fluid quantity.

Xiang and Bousfield (9) explained a further retardation of absorption into large capillaries by the increased drag offered by a forming filtercake of thickness $\boldsymbol{l}(t)$. The filtercake was assumed to form at the interface between ink and coating surface associated with the large volumes of fluid absorbed by larger pores. However, this would also be inconsistent with the faster setting of inks on finer pore structures if it were the only retardational mechanism. They proposed a model for the filtercake formation and this is adopted as an averaging process over the macro-absorption phenomenon. Through filtration, a solids concentration occurs at the boundary to the point of immobilization and subsequently the filtercake formed acts as a porous structure itself progressively becoming much "finer" than the coating and extending in thickness but maintaining a saturation level of liquid. The thickness of the filtercake grows as long as there is free liquid present. After that point the filtercake acts as a competitive structure as menisci form at the drying free surface until equilibrium is found balancing the Laplace pressures of all the involved liquid/vapor menisci. Subsequently, chemical and diffusive mechanisms are expected to become dominant. To apply this model to the dynamic situation in a film split requires that it is possible to define an effective boundary between the immobilized filtercake and the remaining fluid ink

THE RHEOLOGICAL CHARACTERISTICS OF THE FLUIDS AND INKS

During the print process the ink experiences pressure-induced shear and several stages of film splitting where cavitation and filamentation can occur. The breaking length of the filaments depends on the shortness of the ink, a phenomenological term which is important for the printer. In order to achieve an even glossy ink film the microscopic leveling of the broken filaments is crucial. Failure to level can also be recognized sometimes on a macroscopic level as an orange peel effect more well-known in the context of filmpress paper coating. Leveling can happen due to gravity on slow single color presses but more important due to spreading forces if the surface energy of the substrate is high enough and due to the elastic relaxation of the induced film split roughness (11). The process is retarded with growing viscosity due to fluid loss and viscous structure rebuild, through oil removal from the ink by substrate absorption. The latter results in a decreasing mobile ink layer thickness and the overall phenomenological effects are known as the tack build-up of the ink layer.

In order to study the behavior of ink, it is of preliminary importance to examine some of the ink's flow properties. For this purpose a StressTech[4] controlled stress rheometer with a plate-plate system (UP40) was used. The plate-plate system permits the measurement of a wide range of viscosities, due to its adjustable gap which we kept at 0.25 mm throughout this work. Offset-inks consist of a liquid-polymer-solid blend of complex rheological behavior. Our main interest was therefore to analyze the viscosity of the ink as a function of oil loss as experienced in the post-print regime on an absorbent substrate. We chose to use a commercial ink, Skinnex cyan 4x73[5] throughout this work. As concentrating an ink is almost impossible to perform uniformly, we investigated ink dilution. By progressively expanding (diluting) the ink with a standard mineral oil, as used in the formulation of offset-inks (Haltermann PKWF 6/9 af), the influence on steady state shear and subsequent structure rebuild was monitored over time as a complex viscosity $\boldsymbol{h}^*(t)$.

The ink and the oil were mixed thoroughly first by hand using a spatula, then under ultrasonic for 5 minutes and final homogenization on the rheometer devise itself. For the rheological measurements, a steady shear rate of 360 s^{-1} was used for 180 s and, for the tack measurements, a time of 180 s on the IGT distributor was also used for comparative consistency. With our measurement system, high shear rates (> 50 s^{-1}) showed an unstable rheological behavior, probably due to centrifugal loss of fluid/measuring system contact. We applied, therefore, a shear-rate of 30 s^{-1}, avoiding such problems. Furthermore, we wanted to obtain data to model the tack rise as measured with the ISIT device. During the ISIT test procedure, as explained later in some detail, and also in a real printing process, the ink is sheared moderately in the nips of the distributing rollers, then split onto the paper

[4] StressTech is a product name of ReoLogica Instruments AB, Lund, Sweden.
[5] Skinnex is a product name of K+E Inks, Stuttgart, Germany.

where the ”sheared-out” ink structure subsequently starts to relax. During the on-going relaxation, the tack is measured as a function of time after printing.

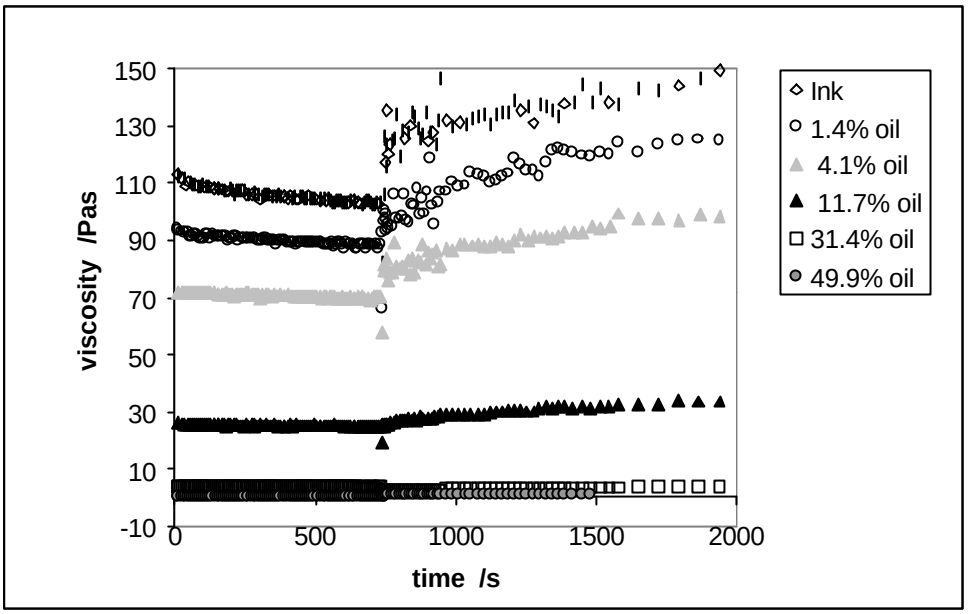

Fig. 1 *Overview of shear viscosity at 30 s^{-1} and subsequent relaxation monitored by stress oscillation in the linear visco-elastic (LVE) regime as a complex viscosity,* ***h*****.*

Fig. 1 shows some experimental results over a range of dilutions. The data from the initial range represents the steady shear experiment. We see the shear thinning of the original undiluted ink over an extended period of time. The shear thinning is progressively less pronounced with increasing added oil content. After relief of the shear stress a structure rebuild occurs as monitored by sinusoidal oscillations of the lowest possible shear (0.5 Pa) or strain in order to remain in the linear visco-elastic domain. The underlying phenomena of the sheared ink relaxation are polymer chain rearrangement and re-establishment of interactions of the solid ink particles and the fluid phase. It has to be noted that in the structure relaxation, in contrast to the steady shear experiment, a complex viscosity is measured which contains an elastic contribution.

The relaxation is seen to obey approximately the relation:

$$h^*(t) = \left(h^*(\infty) - h^*(0)\right) \cdot \left(1 - e^{-t/\hat{o}_0}\right) + h^*(0) \qquad (1)$$

where $\boldsymbol{t}_0$ represents the characteristic relaxation time. Eq. 1 was entered into TableCurve 2D* which fits $\boldsymbol{t}_0$, $\boldsymbol{h}^*(0)$ and $\boldsymbol{h}^*(\infty)$ to achieve the smallest residue r^2. This software is used for all curve fittings throughout this paper. The equation applies well to the measured curves except for the first few data-points where a much faster relaxation process overlays. This initial relaxation may be sample or instrument related. There is evidence of a viscosity drop before recovery and so this could be an inertial effect. However, the first regime lasts only a few seconds. The characteristic relaxation times are seen to trend towards shorter values as the ink oil content decreases. As an example, the blend containing 11.7 w/w% oil is shown in Fig. 2 with a $\boldsymbol{t}_0 \sim 500$ s.

* TableCurve is a product name of SPSS Inc.

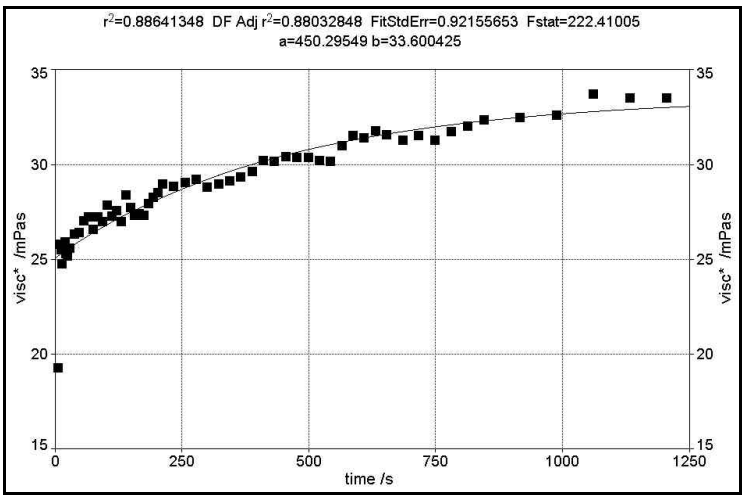

Fig. 2 *Ink structure recovery regime fitted with Eq.1*

The viscosity data for $\eta^*(0)$ are then used as representative values for the subsequent extrapolation to increasing ink solids content, i.e. the regime of oil loss by capillary absorption into the substrate, using an exponential fitting function.

$$\ln \eta^* = a + b\Delta f_{\text{oil}} \qquad (2)$$

where *a* and *b* are fitting parameters and Δf_{oil} is the added oil content in w/w% with respect to the sum of the undiluted ink plus the added oil. The resulting curve is displayed in Fig. 3 with the parameters *a* and *b* shown and the proposed values are used later to compare with the ISIT findings.

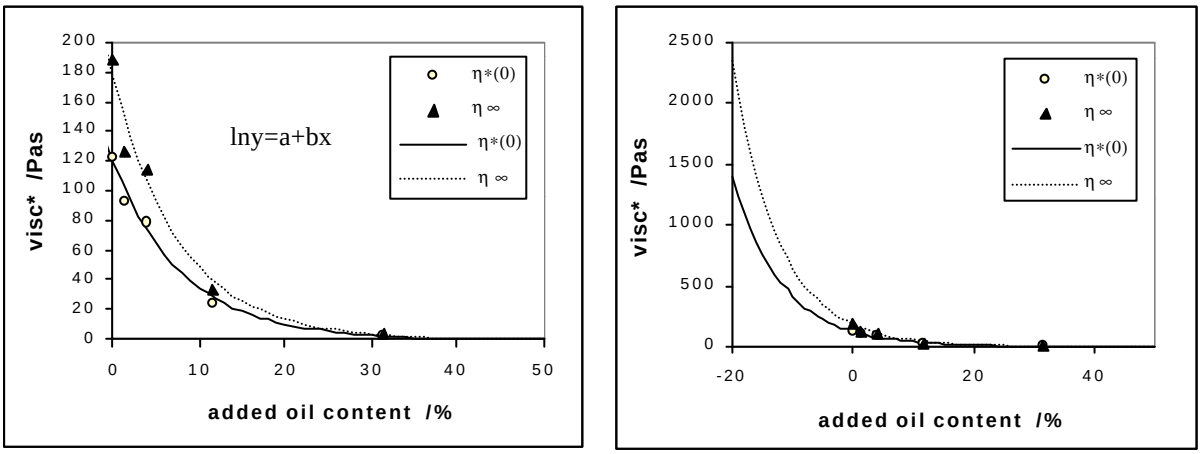

Fig. 3 *Comparison of* $\eta^*(0)$ *and* $\eta^*(\infty)$ *as a function of added oil content of the ink* Δf_{oil} *(w/w%) - the extrapolation of* $\eta^*(0)$ *(a=4.78, b= -0.122) , on the right, to reduced oil content, is used as the basis for the viscosity comparison with ink tack measurements*

THE TACK FORCE DEVELOPMENT OF AN INK FILM ON A SUBSTRATE

Ink-on-paper tack as measured by the ISIT device is defined as the maximum force experienced by a contact disc of material similar to an offset printing blanket separating from a tackifying ink film measured using a solenoid, coil spring and load cell (12). The contact disc is pressed against the print on the sample platen by the electromagnetic force acting on the solenoid. This action applies an extensional force on the coil spring mounted in parallel with the solenoid. Contact time and force can be varied by electronic controls to optimize adhesion between contact disc and print. At cessation of the electromagnetic force the contact disc is retracted from the print by the strain force of the extended coil spring, strong enough to achieve separation of the disc from the ink film. Under small extensions, the coil spring provides a constant acceleration during the retraction of the disc. This is a unique feature of this static test procedure. The strain gauge, fixed between contact disc and coil spring,

generates a load-dependent signal which is recorded as the force during separation as a function of time. The maximum in this force is defined as the tack force at the given time of separation. The sequence is automatically repeated for a pre-defined number of cycles chosen to span the timescale regions of the tack force under study. The build-up of the tensile force required to achieve each individual separation is recorded with time, i.e. the pull-off curve, and can be analyzed through specifically designed software.

The basic physics behind the tack force has been previously described (12). The interpretation, involving both optical examination of the pull-off areas on the printed paper stripe and the tack force curve over time, proposes a rupture at the weakest point of the adhesion/cohesion chain (13), i.e.QUOTEADDIN either between ink and paper or between ink and blanket, or within the cohesive layer of the ink itself.

The surface tension of an ink is not easy to measure in respect to ink wetting and adhesion, because of the reduced mobility. Although the surface tension of the included mineral oil is quite low, the ink itself has a strong contribution from the more polar binders, their solvent agents, e.g. linseed oil, and from the relatively high surface energy of the contained solid particles.

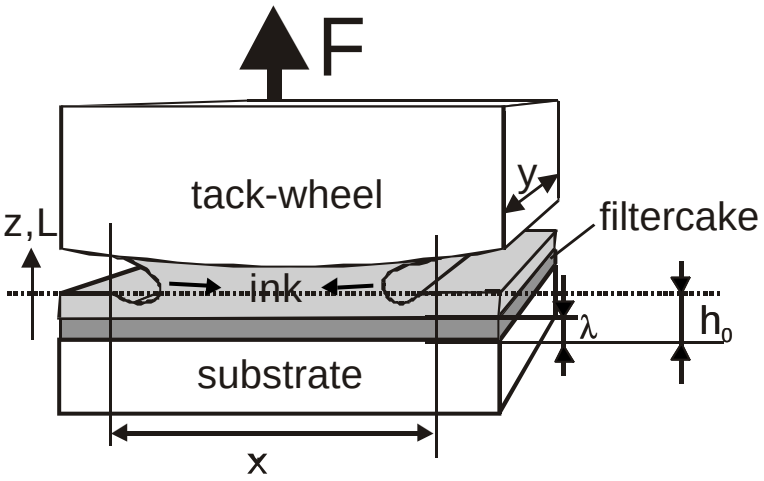

Fig. 4 *Schematic view of tack set-up under the assumed formation of a filtercake with thickness* ***l***

Corresponding to Fig. 4, we introduce here a more comprehensive model as follows in a general form of:

$$F = F_{ad} + F_m + F_{cav} + F_ç + F_i \qquad (3)$$

where F is the force measured on one single pull-off and F_{ad} is the static force due to interfacial tension and, according to Adamson (14), is approximated by:

$$F_{ad} \cong (\gamma_S + \gamma_L - \gamma_{SL})\sqrt{xy} \qquad (4)$$

This is the force, for example, which holds a water drop on a vertical glass surface, where γ_S is the surface energy of the solid, γ_L the surface tension of the liquid and γ_{SL} is the interfacial tension. In the case of two very smooth flat solids, adhesion forces can become appreciable. It is recognized here that pure solid surfaces do not exist in nature. Even a clean crystal immediately after cleavage is covered by adsorbed molecules from the surrounding atmosphere. If this can be prevented, solid surfaces of the same material, which are absolutely smooth and plain, grow together, a process known as “ansprengen” in the optical industry, and in the case of two different crystals as wafer-bonding. In the case of a setting ink, the adhesive boundary force, either to the substrate or to the blanket, contains an additional factor due to the adsorption of the dissolved polymers onto those boundaries.

If there is only liquid between the two solid surfaces we have the additional effect of meniscus formation and retreat exerting a force F_m which is given by (14):

$$F_m = \frac{2\gamma_{LV} xy h_0 \cos\theta}{z^2} \qquad (5)$$

for a given value of z, and furthermore the cavitation phenomenon will exert the force F_{cav} which we will go on to discuss further.

The macroscopic adhesion effect between two surfaces, which, for example, can be observed when separating two large glass plates, has a strong contribution from the underpressure (vacuum) formed as a gap is created between them. This can often be heard and felt as the subsequent airflow occurs into the gap. If, as is the case in our experiment with ink, a fluid with a higher viscosity than air is used, then viscosity and inertia act virtually to glue the plates together. Xiang and Bousfield (9) developed a model based on the separation of parallel plates in a fluid. They related ink viscosity and other dimensional parameters to the force of separation occurring in the remaining fluid ink layer after the proposed filtercake forms. This assumes that the filtercake forms a definable boundary between immobilized ink and that remaining fluid ink layer. The viscous term F_{η} in this case is an extensional term. Keiter (15) solved the Navier-Stokes equation for circular and elliptical plate-plate systems for the viscous contribution and arrived at a fairly similar equation to that which Xiang and Bousfield (9) quote in the form of "Stefan's law" which, however, seems to be dimensionwise inconsistent ($r^2/2$ is missing comparing to Eq. 6). Keiter's derivation is

$$F_{\varsigma} = A\eta u r^2 / 2h^3 \qquad (6)$$

where, r, is the radius of the circular plate, A, the basal contact area, η, the viscosity of the fluid, u, the velocity of separation and, h, the separation distance. In the course of this work we later try to test the application of this equation to our results.

Finally, the whole process is explicitly dependent on the velocity of separation, or more particularly the acceleration. At sufficiently slow separation, no cavitation occurs at all, only menisci form, provided the ink is mobile enough, which retreats with growing distance z and coherent growing radius of the menisci, i.e. one single large filament forms which stretches until it breaks. For high speed separation, inertia due to the mass of the liquid in between becomes important, represented in Eq. 3 as F_{i}, resisting flow and giving rise to cavitation. The most general form of this force may be expressed as Newton's second law of motion acting on a mass, m:

$$F_{i} = \frac{\mathrm{d}^2 z}{\mathrm{d}t^2} m \qquad (7)$$

not taking into account the real flow field in a separating plate process.

Relevant parameters for the ink film separation

Some relevant data for the physical characterization of our tack experiments are given in Table 1

	Symbol	Value	Unit
Ink density	r_i	1.01 x10^3	kgm^{-3}
Printed area	A_p	46.62 x10^{-4}	m^2
Pull-off or footprint area	A_F	5*17 (x*y) x10^{-6}	m^2
Ink mass	m_i		kg
Ink layer thickness	h_0	0.99 x10^{-6} (n=37, ±0.12)	m
Filtercake thickness	l		m
Remaining ink layer under tack measurement	h_T		m
Mobile ink layer thickness	$(h_0 - l)$		m

Table 1 *Symbols, abbreviations and values used in the relevant calculations, n is the number of measurements*

Tack measurements on non-absorbent substrates

The ISIT device provides a means to study some of the mentioned phenomena using the geometry shown in Fig. 4. If not mentioned otherwise, a standard procedure was followed of applying 0.3 ml of ink to the IGT distributor which results in a theoretical 2.4 µm ink layer on the print roller. Performing tack experiments first on different non-absorbing substrates with different surface free energies provides the necessary information about the influence and relevance of the first term F_{ad} assuming that the split is slow enough to ignore inertial terms.

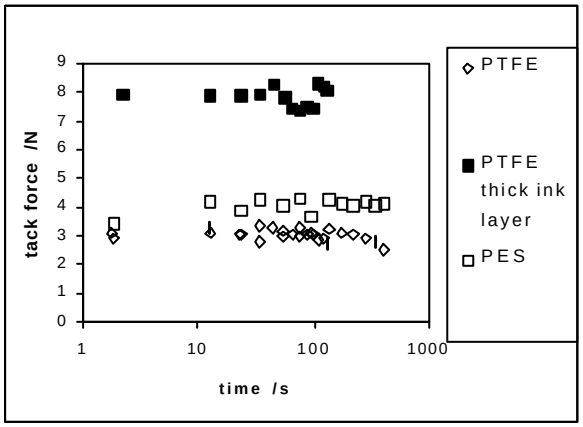

Fig. 5 *Tack curve on smooth substrates.*

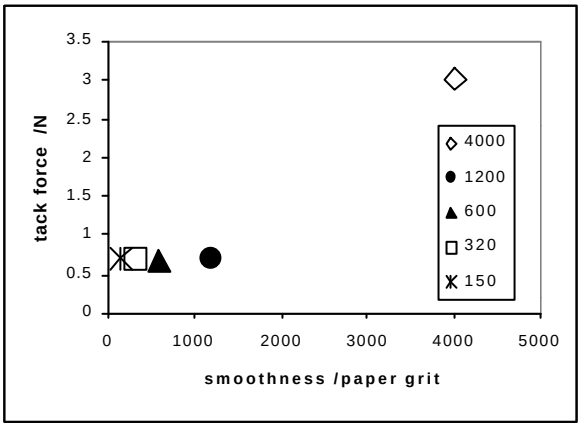

Fig. 6 *Tack force on PTFE in relation to roughness/smoothness. The X-axis shows the sandpaper grit, the value of 4000 is arbitrarily attributed to the untreated smooth surface.*

Results using the two substrates polyester (PES) and polytetrafluoroethylene (PTFE) are shown in Fig. 5. The latter substrate having one of the lowest surface free energies, ~ 18.5 mNm^{-1} (16), of all available technical surfaces. Therefore, F_{ad} is at the lowest possible value. Indeed a microphotograph shows non-wetting, reticulated (spinoidal dewetting), droplets of ink on the PTFE after printing, Fig. 7. From Fig. 5 we even see a continuous

time-dependent decrease of the tack value. This is probably due to the formation of receding droplets, recovering by reticulation from enforced zero contact angle to their naturally higher ones, resulting in less covered surface.

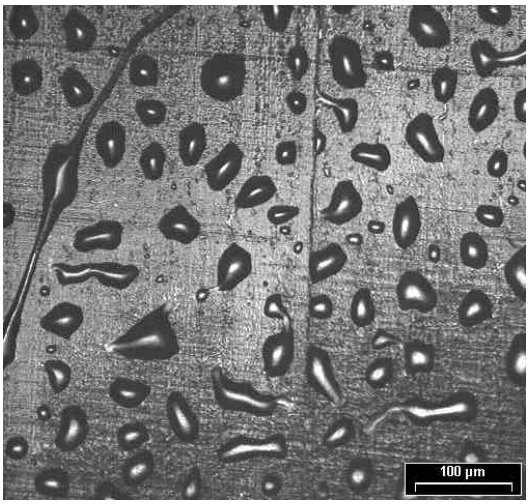

Fig. 7 *Receding ink droplets on PTFE (spinoidal or nucleated dewetting) as seen using confocal laser scanning microscopy in reflected light mode*

It is perhaps unexpected to see a measurable tack value at all, because, following Eq. 4, the value for the interfacial adhesion would be zero or even negative. Therefore the interface PTFE/ink would be the weakest point. Nevertheless, we see that for a very thick coating of ink, ~ 50 µm, obtained from a blade coated PTFE strip, that there is a very high tack reading. This shows clearly that there is no rupture at the weakest point of the adhesion chain but different mechanisms play a dominating role in the case of this very smooth substrate where the continuity of cohesion dominates. We propose that the liquid covering the solid has solely a sealing effect. A forced separation in combination with a liquid of high viscosity causes cavitation while viscoelastic and inertial forces of the ink denoted as F_η and F_i withstand the meniscus equilibrium formation and the retreat. Cavitation means a vacuum within the nucleating voids while the liquid and above-mentioned effects seal this vacuum for a short time period. This ”sucker-effect” acts as a very strong force giving a steep rise in the pull-off force curve, while a second regime of smaller gradient indicates the contribution of the subsequent filamentation under uniaxial elongational viscosity, which in turn is dependent on the amount of stretchable ink available.

A further experiment on PTFE includes samples which have been mechanically roughened by grinding them with different grit sand papers. Fig. 6 shows the mean tack as a function of "roughness". The effect of the introduction of roughness is evident. The ink sits within the scratches constituting the roughness, consequently less ink is in contact with the tack test roller and the sealing effect is reduced. Therefore, a direct relation of roughness and ink layer thickness is evident. If the ink layer is thinner than the average roughness of the substrate, a step down in observed tack behavior may be expected.

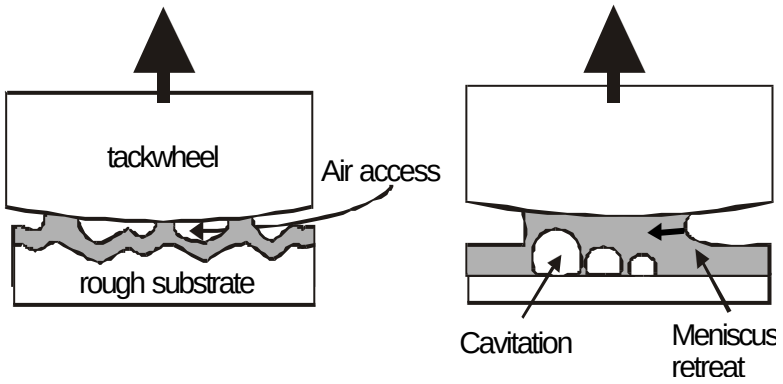

Fig. 8 *Cavitation: on the left, a rough substrate means less ink contact and enables air access, on the right, cavitation at initial fast separation with meniscus retreat as extension progresses, dependent on* ***h***

Tack measurements on paper

We now consider the most relevant case of commercial offset paper (Ikonofix[6] 150 gm^{-2}). The long timescale tack curve cycle shown in Fig. 9 is averaged from more than 30 single tack curves. We recall once again that the long term tack reflects the equilibrium "aging" of ink on a real press and that such timescales are indeed relevant to press runnability.

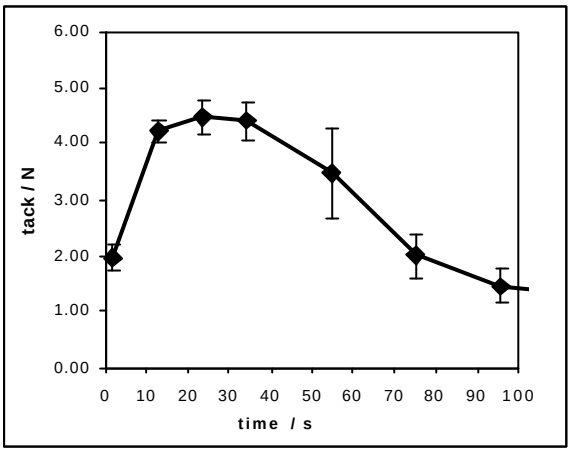

Fig. 9 *Overall mean tack curve for test paper*

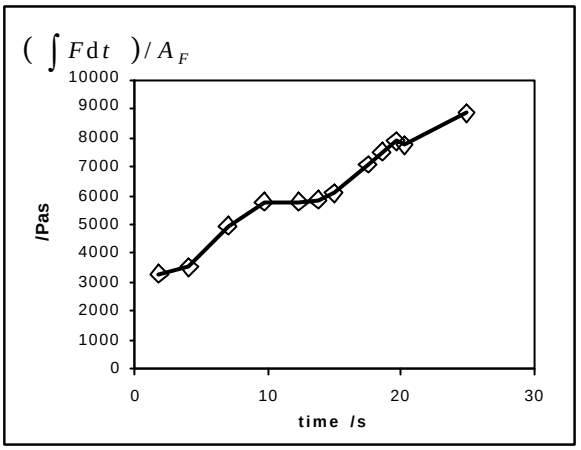

Fig. 10 *The tack rise in the form of a "process viscosity", values are shown in Table 2*

We see that the tack rise is completed for this paper in the order of 30 s. This is the regime of interest with respect to capillary oil imbibition from the initially viscosifying ink layer into the paper. Instead of plotting the force values at the relative coarse time steps shown in Fig. 9, we analyzed the force-time integral, as suggested intuitively by Gane, Seyler and Swan (13), of the single pull-off curves illustrated in Fig. 11, within the tack rise region, given by,

$$\eta_p = \frac{\int F \mathrm{d}\, t}{A_F} \qquad (8)$$

where A_F is the footprint area formed by the contact of the tack wheel with the paper surface. The obtained expression has the units of viscosity, a "process" viscosity, η_p, and is plotted in Fig. 10.

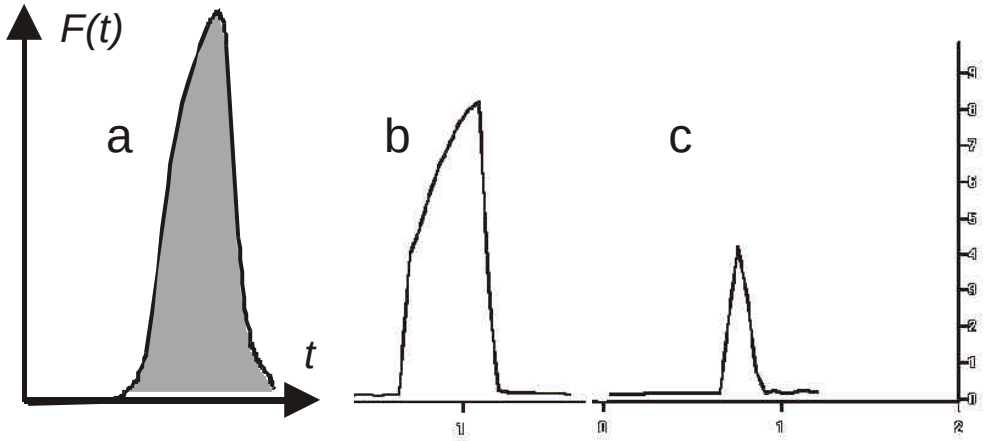

Fig. 11 *a) schematic pull-off curve with integrated area, b) typical curve of Fig. 5 showing 2 regimes: probably cavitational and viscous ones. c) typical pull-off curve as in Fig.10*

[6] Ikonofix is a product name of Zanders Feinpapiere AG, D51439 Bergisch Gladbach, Deutschland

Invoking the filtercake model

In the next step we invoke Eq. 6 to analyze for the proposed phenomenon of filtercake formation during the pull-off integral series in Fig. 10. The filtercake formation is assumed to lead to a decreasing layer thickness of mobile ink.

In order to distinguish the potential effect of viscosity in relation to the mobile ink layer, a test was performed to determine the mobile ink layer thickness as follows.

An ink roller was tared on a microbalance with a resolution of 0.1mg. The ink roller was covered with ink on the IGT distributor device for 60 s. The roller was weighed to determine the applied mass of ink and then transferred to the ISIT device. The test paper strip was printed with one revolution at time $t = 0$ at a speed of 0.5 ms^{-1}. By measuring the weight of ink left on the print roller it was seen that a split ratio of 2, ~ 50:50, was obtained and a mass of printed ink, m_p, was applied onto the paper strip. The value of the starting ink film thickness, h_0, was obtained from the ink density, ρ_i, and the complete area of the print, A_p, using Eq. 9, in which the distribution of the ink layer is assumed uniform:

$$h_0 = \frac{m_p}{\rho_i A_p} \qquad (9)$$

After $t = \Delta t$ seconds, a fresh, uninked, also pre-weighed roller was used to split the ink layer back from the paper and the roller was weighed again. Using Eq. 10, the mass difference, m_{bs}, representing the back-split ink, yielded a mobile ink layer thickness $(h_0 - l(t))$ where the split ratio, R_{split}, for the back splitting was determined from measurements at the shortest times and was found to be 1.18, where a value of 1 would mean all the ink would be removed back onto the roller – this value is assumed to be constant over time as the filtercake grows.

$$(h_0 - l(t)) = \frac{m_{bs} R_{split}}{\rho_i A_p} \qquad (10)$$

The values obtained are plotted in Fig. 12 and a fitting was applied providing a value of $(h_0 - l(t))$ as a function of time using the applied boundary condition of $h_0 = 0.99$ µm, given by the initial 50:50 printing application split, as follows:

$$\ln(h_0 - l(t)) = a + bt \qquad (11)$$

where, once again, a and b are fitted constants. This fitted expression was used as the mobile wet film thickness curve for the subsequent calculations.

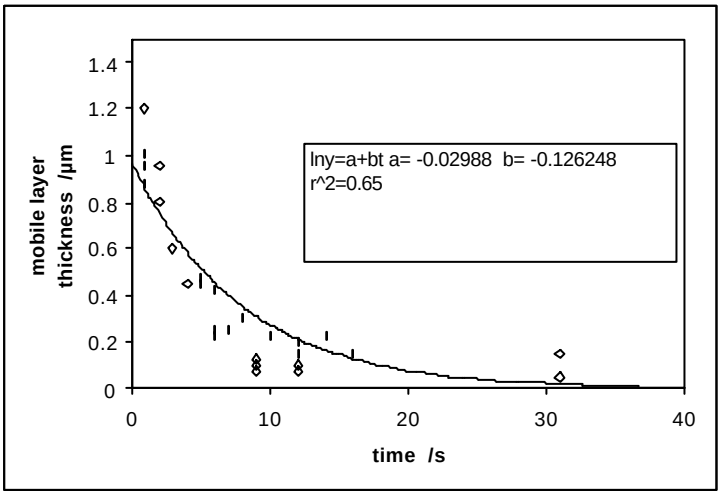

Fig. 12 *Mobile ink layer thickness as a function of time obtained from gravimetric ink splitting experiments*

Invoking the separation of parallel plates, as given in Eq. 6, we now attempt to model the tack response. This approach, however, gives us a decreasing viscosity of the ink as tack increases because the reduction in mobile film thickness occurs so fast, as force is proportional to h^{-3}. This disallows a response from the more slowly varying viscous term. This is considered practically unrealistic, and furthermore it gives results many orders of magnitude away from measured shear viscosities. The results are shown in Table 2.

Balancing the tack-force/footprint area ratio with a process viscous term, η_p, and a dimensionless strain expression, $\gamma(t)$ [~ $x/(h_0 - l(t)$], based on the schematic view of the parameters in Fig. 4, we obtain a different relation. This new relation is not so strongly depending on the mobile film thickness decay, following:

$$\frac{F(t)}{A_F} = \eta_p \frac{d\gamma(t)}{dt},$$

where $$\frac{d\gamma(t)}{dt} = \frac{u(t)}{(h_0 - l(t))}$$

and, therefore $$\int \frac{F(t)dt}{A_F} = \eta_p \gamma(t) = \frac{\eta_p x}{(h_0 - l(t))} \qquad (12)$$

Nonetheless even if we solve this equation for η_p we still obtain a decreasing viscosity as function of time. This could be explained with other dominant phenomena as discussed in the introduction of this section or by questioning the reliability of the obtained values of $(h_0 - l(t))$. The film-splitting technique must assume an immobilized layer which has a distinct boundary condition with the mobile fluid layer under the dynamics of the split. Oil loss is occurring within the region above the proposed filtercake, as well as from the truly mobile layer above this interface. We must conclude, therefore, that there is no well-defined delineation or boundary between the filtercake and the continuously concentrating mobile layer under the conditions of our test. The observed deviation of back split ratio, away from the generally accepted 50:50 assumption, is already an indication that wet adhesion close to the paper surface boundary is not strong enough to maintain the continuity of a filtercake with that surface. This is probably due to air intake into the split from the underlying substrate roughness and porosity. The static pull-off technique offered by the ISIT apparently maintains the continuity between mobile and immobilized ink portions, thus probing the continuous tackification of the ink throughout the cohesive ink layer.

A different method was therefore tried by measuring the print densities on the papers from the splitting test to find a correlation of the remaining ink layer thickness and print density. We then measured the print densities directly on the tack pull-off footprint areas of the tack tested samples used in our short time tack tests (Fig. 10). By comparing the ink film thickness remaining on the paper after backsplitting as a function of print density it is possible to determine the thickness of the layer extended during the independent pull-off measurement of the ISIT, i.e. via Fig. 13 to obtain Fig. 14.

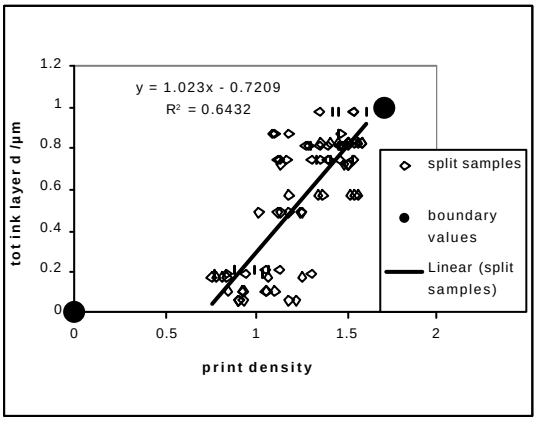

Fig. 13 *Total remaining ink layer thickness as a function of print density*

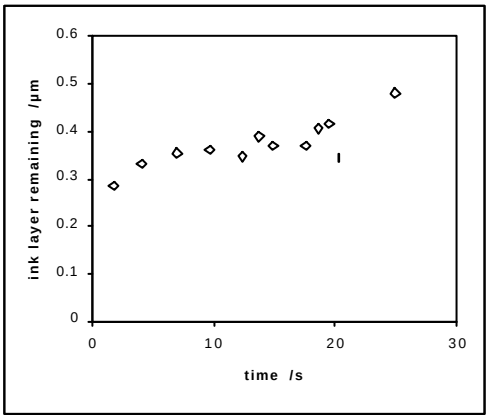

Fig. 14 *Ink layer remaining on paper after tack test as a function of time*

Using the values in Fig. 14 we get a rising viscosity prediction (see Table 2) which confirms that the pull-off test leaves a thinner ink layer than is predicted from a simple filtercake back split model. But this viscosity is still 3 orders of magnitude greater than a measured shear viscosity. This causes us to question the validity of both Stefan's law approximation and similar planar shear expressions involving a distance of separation for typical tack measurements involving very low layer thicknesses and fairly high velocities of separation.

Using an extensional model

The static pull-off mode of the ISIT provides a close approximation to a constant acceleration extensional regime. Going back to Fig. 10, Fig. 4 and Eq. 8, we now consider an uniaxial extensional term as, for example, given by the strain expression (Macosko (17)) in which the extension to a dimension of L occurs from a start dimension of L_0:

$$\varepsilon = \ln(L / L_0) \qquad \textit{Eq. 13}$$

such that the uniaxial extensional viscosity, η_u, can be expressed via the stress tensor, T_{ij},

$$\eta_u = (T_{zz} - T_{yy}) / \dot{\varepsilon} \quad = \quad F(t)e^{\dot{\varepsilon} t} / \left(A_F \dot{\varepsilon} \right) \qquad \textit{Eq. 14}$$

where ε is the Hencky strain. To remove the unknown rate of change of strain, we integrated Eq. 14 with respect to time over the complete single pull-off curve using $F(t)$ as the measured separating force to obtain a process extensional viscosity, η_{pu} .

$$\frac{\int_0^\infty F(t)\,\mathrm{d}t}{A_F} = \int_0^\infty \eta_{pu}\,\dot{\varepsilon} e^{-\dot{\varepsilon} t}\,\mathrm{d}t = \left[-\eta_{pu} e^{-\dot{\varepsilon} t} \right]_0^\infty = \eta_{pu} \qquad (15)$$

The ISIT software provides directly the force-time integrals, so we can obtain η_{pu} directly, confirming the intuitively proposed Eq. 8. We can now match the values with the extrapolated, independently-determined, $\eta^*(0)$ from the relaxation measurements using a scaling via the Trouton ratio,

$$\eta_{pu}(t) = 3\eta_1(t) \qquad (16)$$

which relates the extensional viscosity to the shear viscosity and normalizing $\eta_1(0)$ with $\eta^*(0)$ by a simple scaling factor, k.

The assumptions implicit in the integration made in Eq. 15 are that the effect of changing L_0 is ignored and that L is large when T represents the end of the pull-off, i.e. that $\mathrm{d}\varepsilon/\mathrm{d}t$ is large as the tack wheel finally extends the ink to fracture point. This allows the boundary of the integral in t to be considered as $t \sim \infty$. If this were not the case then Eq. 15 would become,

$$\frac{\int_0^T F(t)\,\mathrm{d}t}{A_F} = \int_0^T \eta_{pu}\,\dot{\varepsilon} e^{-\dot{\varepsilon} t}\,\mathrm{d}t = \left[-\eta_{pu} e^{-\dot{\varepsilon} t} \right]_0^T = \eta_{pu}\left(1 - e^{-\dot{\varepsilon} T} \right) \qquad (17)$$

Practically, L_0 is related to the reduced wet or effective mobile layer. However, the extension of the film is so great, leading in fact to a final fracture of the film, that the ratio L/L_0 is always assumed large over the extent of the pull-off action such that we consider conditions of strong flow only. For thicker layers and slower separation times the change to weak flow might be a complicating factor. However, if we stay in one regime, the scaling factor k can be expected to make a good compensation for this assumption. Development of the instrument to obtain position-sensitive data during the pull-off would allow evaluation of ε and $\mathrm{d}\varepsilon/\mathrm{d}t$. Meanwhile, the information is already present in terms of the value of the experimental separation time, T_S, such that the scaling factor, k, could be related to already known parameters by the expression:

$$k = \left(1 - e^{-\dot{\varepsilon} T_S} \right) \qquad (18)$$

to obtain an estimate for $d\varepsilon/dt \sim 0.6\ s^{-1}$, for a pull-off time of $T_S \sim 0.2$ s and $k \sim 0.11$ (Table 2). This is a subject for further confirmation.

Col.1	2	3	4	5	6	7	8	9	10	11
Data point	Time /s	Pull-off integral ∫Fdt /Ns	Eq. 8 solved for η_{pu} /Pas	mobile layer* after split /µm	Stefan's law‡ solved for η (as given by Xiang and Bousfield) /Pas	Eq. 12 solved for η_P using col.5 /Pas	Eq. 12 solved for η_P using col.9 /Pas	h_T ** /µm	Eq. 8/15 and 16 solved for η_{pu} /Pas	Eq. 8/15 and 16 solved for η_{pu} and normalized † to $\eta^*(0)$ /Pas
1	1.8	0.28	3294.12	0.77	1.52356E-15	509497.89	464437.65	0.29	1098.04	122.65
2	4.1	0.3	3529.41	0.58	6.83356E-16	408363.86	466320.00	0.33	1176.47	131.41
3	7	0.42	4941.18	0.40	3.19114E-16	396490.00	629258.82	0.35	1647.06	183.97
4	9.7	0.49	5764.71	0.29	1.33952E-16	329001.23	726272.24	0.36	1921.57	214.63
5	12.3	0.49	5764.71	0.21	5.00549E-17	236971.88	741998.35	0.35	1921.57	214.63
6	13.7	0.5	5882.35	0.17	3.00626E-17	202646.73	704988.24	0.39	1960.78	219.01
7	14.9	0.52	6117.65	0.15	1.98496E-17	181135.42	760307.29	0.37	2039.22	227.78
8	17.5	0.6	7058.82	0.11	8.55849E-18	150539.54	873667.06	0.37	2352.94	262.82
9	18.5	0.64	7529.41	0.09	6.25175E-18	141537.44	877993.41	0.41	2509.80	280.34
10	19.5	0.67	7882.35	0.08	4.48201E-18	130604.52	907053.88	0.41	2627.45	293.48
11	20.2	0.66	7764.71	0.08	3.38723E-18	117777.35	1004721.88	0.34	2588.24	289.10
12	24.9	0.75	8823.53	0.04	6.49487E-19	73957.40	898014.71	0.48	2941.18	328.52

Table 2 *Comparison of values obtained from different approaches.* mobile layer is determined from splitting experiments. **h_T is the remaining ink layer determined from print densities, † normalizing constant k=0.1117, ‡ Keiter's expression gives results of similar dimensions.*

THE INK RHEOLOGY AS IT SETS – obtaining the solids content as a function of time on the paper

Combining Eq. 2, Eq. 15 and Eq. 16 we obtain an approximation for the oil content in our system as a function of the tack force-time integrals and the footprint area,

$$Df_{oil} \approx \frac{ln\left(\frac{\int F(t)dt}{3A_F} k \right) - a}{b} \qquad Eq.\ 19$$

where k is the scaling factor used in Table 2, a and b are the fitting parameters from the $\eta^*(0)$ as a function of oil dilution given in Fig. 3.

The values are plotted in

Fig. 15 for the tack data of Fig. 10 showing the time dependent decrease in oil content of the ink. Recent work by Rousu and co-workers (8) has shown the initial preferential absorption of mineral oils , while the removal of linseed oil is more retarded. Not knowing the formulation of our ink and the total oil makeup, we assume that at the time of 30 s, which is on the tack force plateau, the largest amount of oil removed from the setting ink is mineral-based.

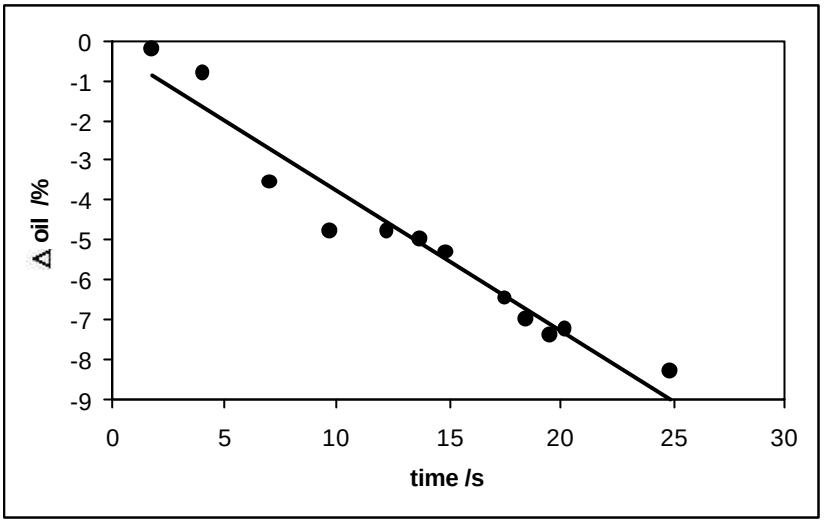

Fig. 15 The proposed differential oil content of the ink from Eq. 19 as a function of time in contact with the paper surface

The fraction of oil content being absorbed by the paper is decreasing linearly with time over the timescale of tack increase (Fig. 15). If we assume the following linearity,

$$D\phi_{oil}(t) = \phi_{oil}(t) - \phi_{oil}(0) = -ct \qquad (20)$$

where $$1/\phi_{oil}(t) = \frac{m_{oil}(t) + m_{solid}}{m_{oil}(t)} = 1 + \frac{m_{solid}}{m_{oil}(t)} \qquad (21)$$

such that, rearranging, we have the mass of oil in the ink as a function of time, $m_{oil}(t)$, in terms of the unchanging mass of solids, m_{solid}, and the original volume fraction of oil, $\phi_{oil}(0)$ in the ink, respectively.

$$m_{oil}(t) = \frac{m_{solid}}{1/\phi_{oil}(t) - 1} = \frac{m_{solid}\phi_{oil}(t)}{1 - \phi_{oil}(t)} = \frac{m_{solid}(\phi_{oil}(0) - ct)}{1 - (\phi_{oil}(0) - ct)} \qquad (22)$$

This is an interesting finding, in that absorption of free fluid over such timescales would normally be expected to follow a $\sqrt{t}$ relationship.

To obtain the rate of mass loss of oil, we can differentiate, to obtain,

$$\frac{dm_{oil}(t)}{dt} = \frac{-cm_{solid}}{[(1 - \phi_{oil}(0)) + ct]^2} \propto -1/t^2 \qquad (23)$$

to find that this rate falls off as t^{-2}.

In this case, the existence of a resistive factor forming as the ink becomes more viscous is the likely explanation. This will need to be tested independently and will be the subject of future work.

CONCLUSIONS

The balance between the interface adhesive and internal cohesive aspects of a fluid layer in contact with surfaces of differing surface energy and roughness has been illustrated using an offset ink and a variety of substrates. It was found that for a non-absorbent smooth surface, the cohesion of the mobile ink film plays the dominant role in respect to the force required to separate a second contacting surface. This was likened to the situation that might occur between two parallel plates in the case where the basal area of one surface is much larger than the other,

such that the ink film can be considered infinite and continuous. This, we conclude, differs in the case of a rough or a porous, permeable surface which would allow the influx of air and rupture at surface discontinuities, in which case the separation force is dominated by viscous, cavitational and, if rapid, inertial forces. Furthermore adhesive forces are important when separation occurs at the boundary layer.

We have shown that it is possible to use tack measurements based on the pull-off technique, as used by the ISIT tester, to determine a model for the viscosity and solids content of an offset ink as the ink begins to set on a paper surface. Under these conditions, the separation force is related predominantly to the viscous properties of the cohesive ink layer. This technique is shown to maintain the cohesion between the wet mobile ink layer and the immobilizing ink-paper interface. Therefore, the concept of a distinct mobile layer existing above that of a delineated forming filtercake is precluded. The continuity between the mobile ink and the concentrating interface is thus maintained and the increase in measured tack is related to the fluid loss and viscosity increase as defined through a uniaxial, extensional viscosity model.

The method developed for correlating the viscosity of an ink, as a function of solids content, with the ISIT pull-off force-time integral provides a potential universal tool for future workers to study the solids and viscosity properties of a wide variety of polymer and particulate suspensions as they interact with the surface of a substrate. It permits the progressive change in fluid properties, for example, through evaporation, absorption, catalysis or external curing, to be monitored in situ.

REFERENCES

1. Gane, P. A. C., Schoelkopf, J., Spielmann, D. C, Matthews, G. P., and Ridgway, C. J., "*Fluid transport into porous coating structures: some novel findings*", Tappi Journal, 85(5), 2000, p1-3

2. Bosanquet, C. M., "*On the flow of liquids into capillary tubes*", Phil.Mag., S6 45(267), 1923, p525-531

3. Washburn, E. W., "*The dynamics of capillary flow*", Physical Review, 17, 1921, p273-283

4. Schoelkopf, J., Gane, P. A. C., Ridgway, C. J., and Matthews, G. P., "*Influence of inertia on liquid absorption into paper coating structures*", Nordic Pulp and Paper Research Journal, 15(5), (2000), 422-430.

5. Bernadiner, M. G., "*A capillary microstructure of the wetting front*", Transport in Porous Media, 30, 1998, p251-265

6. Quéré, D., "*Inertial capillarity*", Europhysics Letters, 39(5), 1997, p533-538

7. Schoelkopf, J., Ridgway, C. J., Gane, P. A. C., Matthews, G. P., and Spielmann, D. C, "*Measurement and network modelling of liquid permeation into compacted mineral blocks*", Journal of Colloid and Interface Science, 27(1), 2000, p119-131

8. Rousu, S., Gane, P. A. C., Spielmann, D. C, and Eklund, D, "*Separation of off-set ink components during absorption into pigment coating structures*", Nordic Pulp and Paper Research Journal, 15(5), 2000, 527-535

9. Xiang, Y. and Bousfield, D. W., "*The influence of coating structure on ink tack development*", Pan-Pacific and Printing & Graphic Arts Conference, CPPA, Canada, 1998, p93-101

10. Toivakka, M., Eklund, D, and Bousfield, D. W., "*Simulation of pigment motion during drying*", Tappi Press, Atlanta, GA, 1992, p403-418

11. Xiang, Y., Bousfield, D. W., Desjumaux, D., and Forbes, M. F., "*The relationship between coating layer composition, ink setting rate, and offset print gloss*", CPPA, 1998, p85-91

12. Gane, P. A. C. and Seyler, E. N., "*Some aspects of ink/paper interaction in offset printing*", Proceedings of the PTS Coating Symposium, Munich,1993.

13. Gane, P. A. C., Seyler, E. N., and Swan, A., "*Some Novel Aspects of Ink/Paper Interactions in Offset Printing*", Printing and Graphic Arts Conference, Halifax, Nova Scotia CPPA, Montreal, Canada, 1994, p209-228

14. Adamson, A. W., "*Physical Chemistry of Surfaces*", A. Wyley Interscience Publication, New York, 1990

15. Keiter, S., "*Haftung und Aufnahme von Druckfarben auf gestrichenen Papieroberflächen*", 1998, Diploma Thesis of the University of Dortmund and Private Communication

16. Van Oss, C. J., Good, R. J., and Chaudhury, M. K., "*The Role of van der Waals Forces and Hydrogen Bonds in "Hydrophobic Interactions" between Biopolymers and Low Energy Surfaces*", Journal of Colloid and Interface Science, 111(2, June 1986), 20-12-1985, p378-390

17. Macosko, C. W., "*Viscous Liquids*", Rheology: Principles, measurements and applications, VCH Publishers, New York, 1994, p425-474